The High Resolution Array (HiRA) for rare isotope beam experiments ⋆

M. S. Wallace [a,*], M. A. Famiano [b,a], M. -J. van Goethem [a], A. Rogers [a], W. G. Lynch [a], J. Clifford [a], F. Delaunay [a], J. Lee [a], S. Labostov [a], M. Mocko [a], L. Morris [a], A. Moroni [e], B. E. Nett [a], D. J. Oostdyk [a], R. Krishnasamy [a], M. B. Tsang [a], R. D. de Souza [c], S. Hudan [c], L. G. Sobotka [d], R. J. Charity [d], J. Elson [d], G. L. Engel [f]

[a] *National Superconducting Cyclotron Laboratory and Department of Physics and Astronomy, Michigan State University, East Lansing MI, 48824*

[b] *Department of Physics, Western Michigan University, Kalamazoo, MI 49008*

[c] *Indiana University Cyclotron Facility and Department of Chemistry, Indiana University, Bloomington, IN 47405*

[d] *Department of Chemistry, Washington University, St. Louis, MO 63130*

[e] *INFN, Milano, Italy*

[f] *Department of Electrical and Computer Engineering, VLSI Design Research Laboratory, Southern Illinois University Edwardsville, Illinois, 62025*

Abstract

The High Resolution Array (HiRA) is a large solid-angle array of silicon strip-detectors that has been developed for use in a variety of nuclear structure, nuclear astrophysics and nuclear reaction experiments with short lived beta-unstable beams. It consists of 20 identical telescopes each composed of a thin (65 μm) single-sided silicon strip-detector, a thick (1.5 mm) double-sided silicon strip-detector, and four CsI(Tl) crystals read out by photodiodes. The array can be easily configured to meet the detection requirements of specific experiments. To process the signals from the 1920 strips in the array, an application specific integrated circuit (ASIC) was developed. The design and performance characteristics of HiRA are described.

Key words: Charged particle detection, Silicon detectors, Silicon strip-detectors
PACS: 29.40.Wk, 28.41.Rc

1 Introduction

The development of unstable rare isotope beams at laboratories such as the NSCL [1], RIKEN [2], GANIL [3] and GSI [4] now permits the study of nuclei far from the valley of beta stability. Experiments with rare isotope beams elucidate the structure of both very neutron-rich and neutron-deficient nuclei and clarify which reactions contribute meaningfully to the nucleo-synthetic r-process or rp-processes within hot or explosive astrophysical environments. Experiments in such facilities will provide meaningful constraints on the isospin dependent interactions within neutron-rich nuclei and neutron stars.

Many of these experiments require reactions to be induced by the most neutron-rich or neutron-deficient isotopes available. Even at the most advanced rare isotope facilities, the available beam intensities for these exotic nuclei are low. To investigate reactions with such beams, it is critical to use a detection system that efficiently covers most, if not all of the interesting kinematically allowable space. The location, in the lab frame, where particles are emitted depends strongly on the reaction mechanism. A variety of silicon strip arrays have been developed to address such needs [5–8]. At low incident energies, where particles may stop in a relatively thin silicon strip-detector, devices such as TIARA [5], which consists of a single layer of silicon have been used for such purposes. With the fast beams produced by projectile fragmentation, however, devices such as LASSA [6], MUST [7] and MUST2 [8] with several layers of detection media have been developed to stop and identify the produced particles. The High Resolution Array (HiRA) belongs to the latter class of strip-detector arrays. It is a highly configurable, highly granular, large solid-angle charged-particle detector with wide dynamic range appropriate for the detection of penetrating reaction products produced at a fast beam facility such as the NSCL [1].

2 Design and performance of the array and its components

HiRA is a modular and expandable array, which currently consists of 20 identical telescopes. Each telescope with an active area of 6.25 cm x 6.25 cm, consists of a 65-micron single-sided silicon strip-detector with 32 strips, a 1.5 mm double-sided (32 x 32) strip-detector, and four 4 cm long CsI(Tl) crystals.

⋆ This work is supported by the National Science Foundation under Grant Nos. PHY-01-10253, PHY-9977707 and by the DOE under grant numbers DE-FG02-87ER-40316 and DE-FG02-88ER-40404

* Corresponding author. Now with Los Alamos National Laboratory
Email address: mwallace@lanl.gov (M. S. Wallace).

It shares many common features with its predecessor, the Large Area Silicon Strip Array (LASSA) [6], and with other devices such as MUST [7] and MUST2 [8]. Figure 1 shows a photograph of 16 HiRA telescopes as they were configured in an experiment designed to measure the proton decays of ^{69}Br fragments produced in the H(^{70}Br,d)^{69}Br reactions at E/A=65 MeV. This arrangement covers laboratory angles out to approximately 30° with a detection efficiency of 60–70%. Three other angular arrangements have been employed in the first series of experiments; each arrangement was designed to optimize coverage for the decay channels studied in the corresponding experiment.

2.1 Mechanical design of a telescope

In each telescope, all detector elements are encapsulated in an aluminum case, which also serves as a Faraday cage. Figure 2 depicts the mounting structure of a single HiRA telescope with the aluminum side panels removed from the top and front sides, revealing a color-coded drawing of the internal structure of the array. The front of the telescope can be viewed as a stack of frames. The first frame (not shown), is a window-frame for mounting the aluminized mylar (or other absorber) foils that are part of the Faraday cage. The next is a collimator frame (red), to prevent low energy particles from stopping in the guard ring structure that surrounds the 6.25 cm x 6.25 cm active area of the first silicon detector. The next frame (green) holds the 65 μm thick single-sided silicon detector. A small frame (light green) follows the single-sided silicon detector, which is slotted to allow insertion of an alpha calibration source. Following the source frame, there is a 1.5 mm double-sided silicon strip detector (blue). Dowel pins align this stack of detectors and frames to each other and to the (orange) frame that follows. Aluminum plates surround this stack, providing additional strength and electronic shielding. The (orange) frame, below the double-sided detector, also supports four CsI(Tl) crystals (green) which are mounted in quadrants behind the silicon detectors. These crystals are 4 cm thick and are trapezoidal with front and back surface areas. Glued to the back of each CsI(Tl) crystal is a 1.3 cm thick light guide (purple) followed by a photodiode (not visable) with active areas of 1.8 cm x 1.8 cm. Directly behind the photodiodes are the CsI(Tl) photodiode preamplifiers. The back panel of the detector has four slots through which the silicon and CsI(Tl) signal cables pass through.

The telescopes were designed such that they can be mounted together using keys which connect the sides of two telescopes. The keys fit along the ridge near the back of the telescopes. As visible on the right side of the photograph in Figure 1, the keys, made of Aluminum, are secured by two screws and are aligned by two dowel pins. The photograph shows how four telescopes were keyed together to form one tower.

Each telescope has one single-sided and one double-sided silicon strip-detector giving a total of 96 (32 x 3) strips. The readout electronics for all these strips is housed in separate boxes which can be mounted inside or outside the vacuum chamber. Mounting the electronics inside vacuum dramatically reduces the number of cables that must be routed through the wall of the chamber. The materials used in the detectors and the electronics have low vapor pressures allowing use in a vacuum chamber with other devices that require vacuum pressures less then a few μtorr.

2.2 Desired performance for various applications

As with other similar devices [7, 8], HiRA is particularly well suited for the studies of light particle transfer reactions in inverse kinematics. Here, we give an example of a neutron pick-up reaction ^{65}Ge(p,d)^{64}Ge at E/A=60 MeV. A heavy beam, ^{65}Ge, impinges on a hydrogen target made of polyethylene foil. A neutron is then transferred to the target creating a deuteron. Figure 3 shows the angular distributions of the differential cross section in the center of mass (top panel) and in the laboratory frame (bottom panel). The deuterons with energy between 10–25 MeV are forward focused in the laboratory frame ($\leq$40 deg). HiRA allows measurements of the center-of-mass frame cross-sections of the emitted deuteron out to large angles with reasonable resolution. For complete kinematics measurements, the missing heavy residue is detected by the S800 spectrometer [9]. The same setup also allows nuclear mass measurement of exotic nuclei by reconstructing the full kinematics of the reaction. However accurate mass measurements require a precise measurement of the incoming beam energy, the reaction angle, and the deuteron energy. Additional detectors systems of time of flight and position-sensitive micro-channel plate detectors have to be developed to measure the beam energy and incoming beam angle [10].

Studies were performed to determine what kind of mass resolution could be achieved using (p,d) reactions utilizing HiRA to measure the energy and angle of the deuteron. Figure 4 shows a simulated excitation spectrum of ^{64}Ge from the ^{65}Ge(p,d)^{64}Ge reaction at E/A=60 MeV. This simulation was based on our measured resolutions in HiRA and the tracking detectors along with anticipated beam rates based on LISE [11]. In this figure one can see the ground state clearly separated with a simulated FHWM of 190 keV. The statistical uncertainty in this measurement would be less then 10 keV. In addition to a ground state mass one can also measure the location of excited states that are separated by more than about 200 keV.

Figure 5 shows the experimental excitation-energy spectrum of ^{6}Li derived from d-α pairs detected in the E/A=50 MeV ^{12}Be+polyethylene reaction

with the HIRA array. The prominent peak is from the 2.186 MeV(J=3+) first excited state of ^{6}Li which has an intrinsic width of 24 keV. Experimentally one measures a FWHM of 150 keV. The black curve shows the result of a simulation of this reaction including the HIRA response, the background (dashed gray curve) and the magnitude of the peak were adjusted to fit the experimental data. Included in the simulations are the energy resolution of the CsI detectors and 1% errors in the energy calibration of each individual CsI detector. The angle uncertainty was given by the Si strip width. A significant contribution to the final width came from small-angle scattering and energy loss of the deuteron and alpha particle in the thick polyethylene target (1 mm). Without these contributions, the simulations suggest one would obtain a FWHM of 117 keV.

2.3 Silicon detector design

The silicon detectors in HiRA were designed by the HiRA collaboration and manufactured by Micron Semiconductor [12]. Several components make up the HiRA silicon detectors: the silicon wafer, its frame, which supports the silicon, and the cabling from the silicon wafer to an external connector. As with its predecessor, LASSA, the HiRA silicon detectors are designed to allow close packed configurations as shown in the photograph in Figure 1 in order to maximize coverage over angular region of interest. It was necessary to design a special frame for the silicon detector as most commercial frames have bulky support structures that prevent close packing.

The schematic drawing of a frame for the single sided HiRA silicon strip-detector is shown in Figure 6. The frame is constructed from G-10 material with an outer dimension of 7.236 cm. An inner ridge supports the silicon wafer, which is epoxied into place. This ridge is recessed into the frame, protecting the silicon and also allowing detectors to be stacked on top of each other. The outer ridge is 2 mm wide and has four through holes, one in each corner, for alignment dowel pins. There is a recessed ledge on one side of the frame where the cable is attached and is recessed enough for wire bonds to stay below the upper surface of the frame. The frames for both thin single sided detectors and thick double-sided detectors have the same external dimensions. However the frame of the double-sided detector has another ridge orthogonal to the first ridge, used for attaching a second cable for the 32 strips on the backside.

In order to read the signals from the detector, a flexible polyimide cable is used. Figure 7 shows a picture of a double-sided Si strip-detector with two connectors, orthogonal to each other. The cables are epoxied to the recessed ridge with a sharp 90 degree bend, allowing the cable to go straight to the back of the detector. On the top of the cable there are gold contact pads,

which allow wire bonding to the silicon surface. HiRA uses three wire bonds from each strip to the cable pad. The cable is 0.246 mm thick. At the other end of the cable there is a small printed circuit board, which connects to a standard 0.1 inch spacing 34-pin Amp female header. The cable is epoxied to the PC board and the traces are soldered on. There are 32 strips on a surface, which connect to traces going to pins 2 through 33 of the connector. Pins 1 and 34 are used to connect the back plane of the single sided detector to the ground. On the double-sided detector these pins do not connect to the silicon wafer.

There are two different types of silicon detector in a typical HiRA telescope. One is a single sided thin (65 μm) detector and the other is a thick (1.5 mm) double-sided detector. The thin detector is denoted "ΔE" as it is used to measure the energy loss by the particle passing through the detector. The other thicker silicon detector is denoted as the "E" detector. For energetic particles that pass through both detectors, the energy deposited in the E detector can be combined with that measured in the ΔE to get total energy loss. Particle identification can be obtained from plotting ΔE vs. E or ΔE vs. Time of Flight.

The E detector and ΔE detector carry the catalog designation BB7-65 and BB7-1500 respectively. The detectors are made of bulk n-type silicon with P+ implantation to form the junction near the front. The surfaces of both detectors have an active area of 6.25 cm x 6.25 cm. There are 32 strips on the front (junction) side of the ΔE detector and E detector with a strip pitch of 1.95 mm. There is a gap of 25 μm between active strips and between the outlying guard ring structure and active strips. The guard ring structure consists of ten concentric rings around the strips taking up 2 mm on all sides. The ten rings are all floating with respect to the front or back voltages. This structure was added to reduce the surface leakage current, particularly on the end strips. The HiRA silicon detectors typically run with leakage currents below 1 μA for ΔE detectors and 1-3 μA for the E detectors at room temperature.

On the back (ohmic) side of the ΔE detector is a single aluminum electrode. The E detector (as shown in Fig 7) has 32 strips on the back (ohmic) side. These strips are perpendicular to the strips on the front side. The pitch on the back of the E detector is also 1.95 mm but it has an inter-strip gap of 40 μm as opposed to the 25 μm on the front. With strips on both sides an effective pixel, based on the strips hit on the front and the back, can be created. If the detector is mounted 35 cm from the target, which is the designed distance, the angular resolution is 0.15°. There is no guard ring structure on the back, which is at ground while voltage is applied to the front during typical experimental setups.

Table 1
The energy resolution for the five strongest peaks in Fig. 7 given raw and after subtracting electronics noise

α Energy [MeV]	FWHM [keV]	FWHM$_{corr}$ [keV]
5.423	31.6	26.6
5.685	33.4	28.7
6.288	33.2	28.4
6.778	35.2	30.7
8.784	33.8	29.1

2.4 Specification and performance of the silicon detectors

All detectors were tested and resolution for each strip was measured prior to use in an experiment. The detector is placed inside a vacuum chamber with no foil between the detector surface and an α source. A 1.2 μCi ^{228}Th source with a thin 50 μg/cm^2 gold window was used. The ^{228}Th source is a very nice calibration source as it contains eight different energy alpha particles with substantial intensity. More than 100 keV separates five of these alphas. This makes them very easy to fit and extract the peak location and full width half maximum (FWHM). The highest alpha energy is 8.7 MeV giving a larger signal than the ^{241}Am source, which has the most intense peak at 5.5 MeV.

The source was placed approximately 20 cm from the detector, illuminating all strips. Because the source-detector distance was less than the 35 cm, the collimation of the guard ring was not effective. Particles striking the guard ring generate signals with reduced energy on the edge. For this test, we used conventional electronics and the detectors were connected to individual pre-amplifiers attached to the scattering chamber on the outside. (These pre-amplifiers were originally built for LASSA and are discussed in Reference 6.)

Figure 8 is a spectra for an average EF strip, where EF refers to the front strips of the E detector and EB refers to the back strips. A Gaussian fit is performed for each peak excluding the low energy tail, which is non-Gaussian for alpha particles. There is also a pulser peak around 14 MeV which is used to measure the electronic component of the overall resolution. Table 1 gives the FWHM resolution for each of the alpha peaks as they were measured and the intrinsic (FWHM$_{corr}$) values, where the electronic noise contribution is subtracted in quadrature. The overall resolution is then taken to be the average resolution of the 5 strongest alpha peaks. For the strip shown in Figure 8 the intrinsic energy resolution is 28.6 keV FWHM.

Particles with higher energy, that will punch through the 1.5 mm Si detector, are detected in the CsI(Tl) scintillation crystals. CsI(Tl) was chosen as the stopping material as it has reasonable energy resolution, can be machined to appropriate dimensions, is far less hygroscopic than other crystals such as NaI, and has a light output well suited for photodiode readout. The CsI(Tl) detectors used in HiRA were manufactured by Scionix. Figure 9 shows a schematic side and front view of the CsI(Tl) crystals used in HiRA. The trapezoidal crystals are 3.5 cm x 3.5 cm on the front and 3.9 cm x 3.9 cm in the rear with a thickness of 4 cm. Behind each crystal is a 3.9 cm x 3.9 cm x 1.3 cm light guide which has been attached using BC 600 optical cement. A 1.8 cm x 1.8 cm silicon photodiode was glued to the photodiode with RTV615 silicon rubber glue. Each crystal is individually wrapped in cellulose nitrate membrane filter paper. The four crystals are then wrapped together with Teflon tape. The front surface of the crystal array is covered with aluminized Mylar foil. The light guides were painted with BC-620 reflective paint.

All the HiRA CsI(Tl) crystals have light output uniformity of 1% for 5.486 MeV particles from an ^{241}Am source [13]. Details of the uniformity test are described in ref. 13. In the same study, it was found that light output non-uniformities in the HiRA CsI(Tl) crystals due to smooth variations in the thallium doping concentration can be corrected. In addition to these smooth variations in light output, local non-uniformities in light output at the level of 0.3% are present in our crystals. No process has been identified so far that can eliminate or remove them.

3 Electronics for the array

The HiRA device consists of 1920 individual silicon strips and 80 CsI(Tl) crystals whose signals must be amplified and digitized. The CsI(Tl) readout uses CAMAC based electronics that were developed earlier for the LASSA device [6]. The application of traditional electronics, where each strip has a discrete pre-amplifier, shaper, discriminator, TDC channel, and ADC channel, to the readout of the HiRA silicon detectors would cost on the order of one million dollars to implement. A lower cost electronics solution is required for HiRA and for other large strip-detector arrays being developed for nuclear, particle, and space-based physics. The implementation of the HiRA Application Specific Integrated Circuit (ASIC), called the HINP16 within the HiRA readout electronics, is described below. A more detailed description of ASIC functionality is presented in a separate paper [14].

3.1 CsI(Tl) readout electronics

Each HiRA CsI crystal is associated with its own pre-amplifier board located within the telescope (see Figure 2). Individual pre-amplifier circuits are removable for easy replacement. Photodiodes attached to the CsI light guides are connected directly to the pre-amplifier circuits. These circuits are mounted to a small board within a single telescope which provides routing to and from each pre-amplifier for power, signals, and test signal inputs. Connection to this common board is via a 16-pin Amp connector. Each telescope is then routed to a common circuit box located near the array; four telescopes are connected to a single box so that 16 output signals are routed to external CAMAC Pico System shaper/discriminator modules via a 34-pin ribbon cable [15]. Output from the variable gain shaping amplifiers was routed to CAEN V785 VME ADCs; each 32 channel ADC accommodates two Pico modules [16]. ADC gating and readout triggering from events in the CsI is possible via a common discriminator OR signal from the discriminator portion of the CAMAC modules or from a discriminator multiplicity output. In the case of a readout trigger other than that of the CsI (e.g., triggering via events in the silicon detectors), only the shaper modules are necessary, as gating of the peak sensing ADCs can be via this trigger.

External electronics for the CsI readout of the entire array consists of 5 16-channel shaper/discriminator modules and three 32-channel peak-sensing ADCs.

3.2 Application Specific Integrated Circuit (ASIC)

The HiRA detector is designed to be a versatile device that can be used in a variety of ways for different types of experiments. For some experiments the energy deposited in the silicon detector is of the order of 50 MeV with particle multiplicities of 1 per event. Some require timing resolutions around 1 ns, others require energy depositions around 500 MeV with particle multiplicities greater than 20. This makes designing a single ASIC difficult; as the name suggests they are application specific. The HiRA ASIC contains charge sensitive amplifiers, discriminators, shaping amplifiers, time to analog converters, and a sample and hold circuit along with the digital logic necessary for communication and multiplexing the signals out. There are 16 individual channels within each chip. Figure 10 is a block diagram representation of the functionality of the HiRA ASIC chip. The ASIC is fabricated in the AMIS 0.5 μm, N-well CMOS, double-poly, triple-metal high-resistance process through MOSIS [17].

The first element of the ASIC, the charge sensitive amplifier (CSA) consists

of two different amplifiers as well as the option to bypass it completely. User selectable CSAs allow for high and low gain settings to accommodate various detector applications. The low gain CSA gives a linear dynamic range of about 500 MeV in silicon. The high gain setting allows particles up to about 100 MeV. in silicon The CSA takes up a large physical area on the chip as a large input MOSFET is required to achieve the required resolution. If a larger gain is required, then the chip be connected to an external pre-amplifier by bypassing the on-board CSAs.

After the CSA or external pre-amplifiers the signal is split with one signal going into the Nowlin pseudo constant-fraction discriminator (CFD) [18, 19]. The discriminator consists of a zero-cross discriminator and a leading edge discriminator. It is the latter which sets the threshold. The other signal is routed to a shaping amplifier, producing an approximately Gaussian shaped signal, with a shaping time of about 1 μs. The signals can be positive or negative. The shaper is a unity gain amplifier so all the chip gain comes from the CSA.

The discriminator has a trigger threshold controlled by an internal digital-to-analog converter (DAC), which can be set both positive and negative for either input level for each of the 16 channels individually. The discriminator output has three functions, start a time-to-voltage converter (TVC), update a hit register, which can be used to determine trigger criteria, and initiate a peak search. When a discriminator fires, the shaped signal will go through a peak find circuit and the peak value will be held until it is read out or forced clear. The time-to-voltage converter (TVC), which has two time range settings of about 150 ns and 1 μs, is stopped by an external common stop signal. The peak of the time signal is then stored until it is read or forced clear.

Each ASIC has a computer controlled external output of the signal after the CSA, after the shaper, and the discriminator logic signal as denoted by solid black circles on Fig. 10. For details on the ASIC see Ref. 14.

3.3 Implementation of the HINP16 within the HiRA readout electronics

The HiRA silicon detectors have 32 strips per surface; so two ASICs are needed per surface. The ASICs are mounted on chipboards in pairs along with other components. Figure 11 shows one of the chipboards with two ASIC chips on it. Below the chipboard is a 4 channel prototype chip with the cover off exposing the actual ASIC. A US quarter coin is placed next to it for size comparison. Additionally on the chipboard are bias resistors and decoupling capacitors for the bias voltage going to the detectors as well as a complex programmable logic device (CPLD) to mediate internal and external chip logic. There is

also a differential-amplifier for the Energy and Time signals. These signals are multiplexed out of the chips and into the differential amplifier generating a differential signal between -1 V and +1 V.

One chipboard is required for each surface of silicon; therefore three are used for each telescope. An additional circuit board called the motherboard is used to simultaneously provide power and serial logic signals to several chipboards and multiplexing functions for sampled signals. The first experiments with HiRA utilize detectors aligned in towers of up to 5 detectors. A motherboard was built that can accept 16 chipboards, which are needed for a tower of up to 5 telescopes.

The motherboard contains a field programmable gate array (FPGA), and level translators between the external control logic and the FPGA and the other circuits on the chipboards. The FPGA is used to communicate with up to 32 chips on the 16 chipboards that the motherboard can service. For each motherboard there are two linear outputs. One contains the sequence of energy values for all channels that have a valid hit register event. The other carries the corresponding time values from the TACs. In addition to this, there is logic information coming out on a high-density logic control cable to communicate the address of each energy and time value sent out from the motherboard.

Each motherboard has three separate computer controlled logic OR signals such that any number of the chipboard OR signals can be set in any combination. There are also three Sum signals, which are also set via computer control. The Sum signal represents an analog level based on the multiplicity. There are six linear inputs for pulsers. They are divided into three for even channels and three for odd channels. Jumpers on the motherboard steer these pulser inputs to specific chip boards slots.

Aside from the motherboard, one only needs two VME modules to handle all information with the electronics. The first is a SIS3301 105 MHz sequencing ADC that contains 4 pairs of sampling ADCs [20]. Each motherboard uses one pair from the sampling ADC. The connection from the motherboard to the ADC is via a dual lemo cable. There is an external clock input that tells the ADC when to sample each of the four pairs. The control of the readout and the storing of addresses from each motherboard along with the ADC clock are handled by an XLM80 universal logic module made by JTEC [21]. The XLM80 contains an additional FPGA, which is programmed with the trigger logic sequences for the silicon detectors.

The ASICs were designed to run in sparse readout, in which a discriminator signal sets a hit register for a specific channel. The hit register bit is then required for readout of that channel to occur. This is highly desirable as otherwise the readout time for an entire tower can be quite long. There

are situations where one might want to force-read electronic channels that did not trigger their discriminators. For this reason software was developed to force the discriminators on all channels to trigger, initiating a full read of all detectors connected to this motherboard.

4 Calibration and particle identification

The HiRA device provides the possibility to perform precise measurements of direct reactions, two- and multi-particle correlations and resonance spectroscopy using both stable and rare isotope beams. The accuracy of such measurements, however, depends significantly on the accuracy with which HiRA can be calibrated in mass, charge, energy and angle. Here we describe how the device was designed to allow accurate measurements of the energy, charges and masses of the various species. In another article, we describe a Laser Based Alignment System (LBAS) that was developed to determine the location of each strip relative to the target [22].

When two layers of silicon are used, the design allows the insertion of a pin source to calibrate the 1.5 mm detector without having to first remove the 65 μm detector. Since the light output of the CsI(Tl) scintillator is particle dependent, the calibration of the CsI(Tl) detector requires beam particles and a precision pulser. Mass and charge identification can be easily obtained from the correlation between the energy loss and the total energy of the particle.

4.1 Calibration of Si detectors with external source

In general, the first layer of silicon can easily be calibrated by placing an alpha source at the target location. The same procedure used to determine the energy resolution of the detector is adopted. The alpha decay peaks shown in Figure 14 are used to calibrate each strip of the detectors. To monitor any gain shift during the experiment, we took data with alpha source when beams were not available.

4.2 Pin source calibration

For experiments with telescopes each of which contains two silicon detectors, the second one is completely behind the first. This makes access to the second detector difficult in order to calibrate using alpha sources. To minimize the handling of silicon detectors, mounting and dismounting them, during alpha

source calibrations, a slot is designed on one side of the silicon box as shown in Figure 12 to fit a calibration source between the silicon detectors. It allows a thin frame, with an alpha source on a pin, to slide between the silicon detectors.

Figure 13 is a picture of one of these source frames. The pin is a 0.5 inch long dowel pin. This pin is activated by electroplating the tip with daughter nuclei from a ^{228}Th source. The source can be generated in 24 hours or less. The unactivated side of the pin is then glued onto the frame as shown in Figure 13. There are three strong alpha lines from this source at 8.785 MeV, 6.050 MeV, and 6.089 MeV. The primary deposition on the pin is ^{212}Pb isotope which have a half-life of 10.6 hours. As there is no additional material between the radioactive nuclei and the surface this source can produce very sharp energy spectra as shown in Fig. 14.

The pin source is capable of hitting all pixels on the E detector as shown in Figure 15. Due to the close proximity to the silicon surface, about 3 mm, the alpha particle strikes the surface with large oblique angles for pixels that are not near the center. The dead layer on the surface of the silicon will shift the energy of the alpha particles and diminish the energy resolution. If there is enough data from reactions with the beam, one can calibrate using only the pixel or pixels directly in front of the pin source, thus avoiding problems with angle and dead layer measurements.

Given the nature of double-sided silicon detectors it is possible to calibrate the energy for all strips if one can accurately calibrate a single strip on the front surface and the back surface. For example, using the pin source, Strip 16 on the front and back are calibrated. Figure 14 is a histogram of strip 16 on the front surface of an E detector taken with a pin source inserted between the ΔE detector and E detector. This histogram is gated on events with only one coincidence hit on both front and back strips. Requiring a signal in strip 16 on the back, effectively selecting alpha particles that hit the central pixel, 16-16. This pixel should have zero incident angles giving the most accurate energy measurement. The two high intensity alpha peaks are fitted, and a linear calibration is done for these two strips. New parameters are then generated with strips 16 on EF and EB calibrated in MeV.

For every particle incident on the silicon, the energy is measured in one strip on the front, and one strip on the back regardless of where the particle hits the surface of the detector. The energy measured by each of these strips should be exactly the same. Thus all particles incident on EF16 can be used to calibrate the corresponding EB strips.

4.3 CsI(Tl) calibration

Since the light output of CsI(Tl) crystals are particle dependent and non-linear, the calculation has to be performed for each isotope of interest. In one of the HiRA experiments, a mixed beam of p, d, t at 86.1, 44.53, and 29.93 MeV at Bρ=1.3716 Tm, was produced from the NSCL coupled-cyclotron-A1900 [23–25]. The beams scattered off elastically from a Au target of 20 mg/cm^2 effective areal thickness. To increase statistics in the extraction of the elastically scattered peak, all the strips in the E detectors are calibrated and a particle identification spectra similar to Figure 16 are generated. Figure 17 shows the peaks of the three hydrogen isotopes, p, d, and t. The peaks are rather sharp and form a nearly linear function between the ADC channel and the particle energy. For experiments where more than the hydrogen isotopes are detected, calibrations with many cocktailed beams and preferably with isotopes of different energy range will be needed.

4.4 Particle identification

Of critical importance in a detection array such as HiRA is the ability to identify the masses and charges of various particles, as well as energy of various particles to an excellent degree of resolution. For particle identification, HiRA relies on the technique of energy loss, ΔE vs E identification. There are two types of ΔE vs E plots that are used to identify particles detected with HiRA depending on the particle energy. For high-energy particles that penetrate into the CsI detectors the second Si detector is used as a ΔE detector, with the particle stopping in the CsI, which is labeled as the E detector. Figure 16 is a ΔE-E plot for particles produced by the fragmentation of a ^{40}Ca beam impinging on a plastic target. One can see lines corresponding to p, d, t hydrogen isotopes as well as lines corresponding to ^{3}He and ^{4}He.

If the energy of particles is lower, then the particles stop in the second silicon detector. In this case the ΔE detector measures ΔE and the second Si detector gives the residual energy. Figure 18 represents the corresponding ΔE-E plot obtained in the beam described above.

Clearly HiRA can identify both the charge number (Z), and the mass number (A) for light charged particles. Up to this point, no data has been measured for heavier fragments. However based on our experience with the LASSA array, HiRA is expected to have particle identification up to oxygen isotopes.

5 Summary

A new charged particle array has been built and characterized. To date the array has been used to perform five different experiments. In these experiments the detectors were arranged in four different physical configurations, showing the devices versatility and usefulness for studies of rare isotope research.

References

[1] MSUCL-939, The K500 $\otimes$ K1200, A coupled cyclotron facility at the National Superconducting Cyclotron Laboratory, The K500 $\otimes$ K1200, A Coupled Cyclotron Facility at the National Superconducting Cyclotron Laboratory (July 1994).

[2] T. Kubo, M. Ishihara, N. Inabe, H. Kumagai, I. Tanihata, K. Yoshida, The RIKEN radioactive beam facility, Nucl. Instr. and Meth. B **70** (1992) 309–319.

[3] W. Mittig, The spiral project at GANIL and future opportunities, J. Phys. G **24** (1998) 1331–1339.

[4] H. Geissel, P. Armbruster, K. H. Behr, A. Brünle, K. Burkard, M. Chen, H. Folger, B. Franczak, H. Keller, O. Klepper, B. Langenbeck, F. Nickel, E. Pfeng, M. Pfützner, E. Roeckl, K. Rykaczewski, I. Schall, D. Schardt, C. Scheidenberger, K.-H. Schmidt, A. Schröter, T. Schwab, K. Sümmerer, M. Weber, G. Münzenberg, T. Brohm, H.-G. Clerc, M. Fauerbach, J. J. Gaimard, A. Grewe, E. Hanelt, B. Knödler, M. Steiner, B. Voss, J. Weckenmann, C. Ziegler, A. Magel, H. Wollnik, J. P. Dufour, Y. Fujita, D. J. Vieira, B. Sherrill, The GSI projectile fragment separator (frs): a versatile magnetic system for relativistic heavy ions, Nucl. Instr. and Meth. B **70** (1992) 286.

[5] W. N. Catford, C. N. Timis, M. Labiche, R. C. Lemmon, G. Moore, R. Chapman, The TIARA array for the study of nucleon transfer reactions, in: Applications of Accelerators in Research and Industry: 17th Int'l. Conference, American Institute of Physics, 2003, pp. 329–332.

[6] B. Davin, R. D. de Souza, R. Yanez, Y. Larochelle, R. Alfaro, H. S. Xu, A. Alexander, K. Bastin, L. Beaulieu, J. Dorsett, G. Fleener, L. Gelovani, T. Lefort, J. Poehlman, R. J. Charity, L. G. Sobotka, J. Elson, A. Wagner, T. X. Liu, X. D. Liu, W. G. Lynch, L. Morris, R. Shomin, W. P. Tan, M. B. Tsang, G. Verde, J. Yurkon, Lassa: a large area silicon strip array for isotopic identification of charged particles, Nucl. Instr. and Meth. A **473** (2001) 302.

[7] Y. Blumenfeld, F. Auger, J. E. Sauvestre, F. Maréchal, S. Ottini, N. Alamanos, A. Barbier, D. Beaumel, B. Bonnereau, D. Charlet, J. F. Clavelin, P. Courtat, P. Delbourgo-Salvador, R. Douet, M. Engrand, T. Ethvignot, A. Gillibert,

E. Khan, V. Lapoux, A. Lagoyannis, L. Lavergne, S. Lebon, P. Lelong, A. Lesage, V. L. Ven, I. Lhenry, J. M. Martin, A. Musumarra, S. Pita, L. Petizon, E. Pollacco, J. Pouthas, A. Richard, D. Rougier, D. Santonocito, J. A. Scarpaci, J. L. Sida, C. Soulet, J. S. Stutzmann, T. Suomijärvi, M. Szmigiel, P. Volkov, G. Voltolini, MUST: A silicon strip detector array for radioactive beam experiments, Nuclear Instruments and Methods in Physics Research A 421 (1999) 471–491.

[8] E. Pollacco, E. Atkin, F. Auger, P. Baron, J. P. Baronick, Y. Blumenfeld, A. Boujrad, A. Drouart, P. Edelbruck, L. Lavergne, L. Leterrier, L. Olivier, B. Raine, A. Richard, M. Rouger, P. Roussel-Chomaz, F. Saillant, M. Tripon, E. Wanlin, MUST II: Large solid angle light charged particle telescope for inverse kinematics studies with radioactive beams, in: J. L. Duggan, I. L. Morgan (Eds.), AIP Conf. Proc. 680: Application of Accelerators in Research and Industry, 2003, pp. 313–316.

[9] D. Bazin, J. A. Caggiano, B. M. Sherrill, J. Yurkon, A. Zeller, The S800 spectrograph, Nucl. Instr. and Meth. B **204** (2002) 629.

[10] D. Shapira, T. A. Lewis, L. D. Hulett, A fast and accurate position-sensitive timing detector based on secondary electron emission, Nucl. Instr. and Meth. A **454** (2000) 409.

[11] D. Bazin, O. Tarasov, M. Lewitowicz, O. Sorlin, Nucl. Instr. and Meth. A **482** (2002) 307–327.
URL `http://www.nscl.msu.edu/lise`

[12] Micron Superconductor LTD, 1 Royal Buildings,Marlborough Road, Lancing, Sussex BN158UN, England.

[13] M.-J. van Goethem, M. S. Wallace, B. E. Nett, M. A. Famiano, K. R. Herner, D. J. Oostdyk, M. Mocko, W. G. Lynch, M. B. Tsang, P. Schotanus, J. Telfer, H. L. Clark, A. Moroni, R. D. de Souza, L. G. Sobotka, Investigatinos and corrections of the light output uniformity of csi(tl) crystals, Nucl. Instr. and Meth. A **526** (2004) 455–476.

[14] G. L. Engel, M. Sadasivam, M. Nethi, J. M. Elson, L. G. Sobotka, R. J. Charity, A multi-channel intergrated crcuit for use in low and intermediate energy nuclear physics - HINP16C, Nucl. Instr. and Meth. A doi:10.1016/j.nima.2006.12.052.

[15] Pico Systems, 534 Lindeman Rd. Kirkwood, MO 63122.

[16] CAEN Technologies, Inc 1140 Bay Street, Suite 2C, Staten Island, NY 10305.

[17] MOSIS, 4676 Admiralty Way, 7th Floor Marina del Rey CA 90292-6695.

[18] C. H. Nowlin U.S.Patent No. 4,443,768 (April 17, 1984).

[19] C. H. Nowlin, Low-noise lumped-element timing filters with rise-time invariant crossover times, Rev. of Sci. Instr. **4** (1992) 2322–2326.

[20] SIS GmbH Harksheider Str. 100A 22399 Hamburg, Germany.

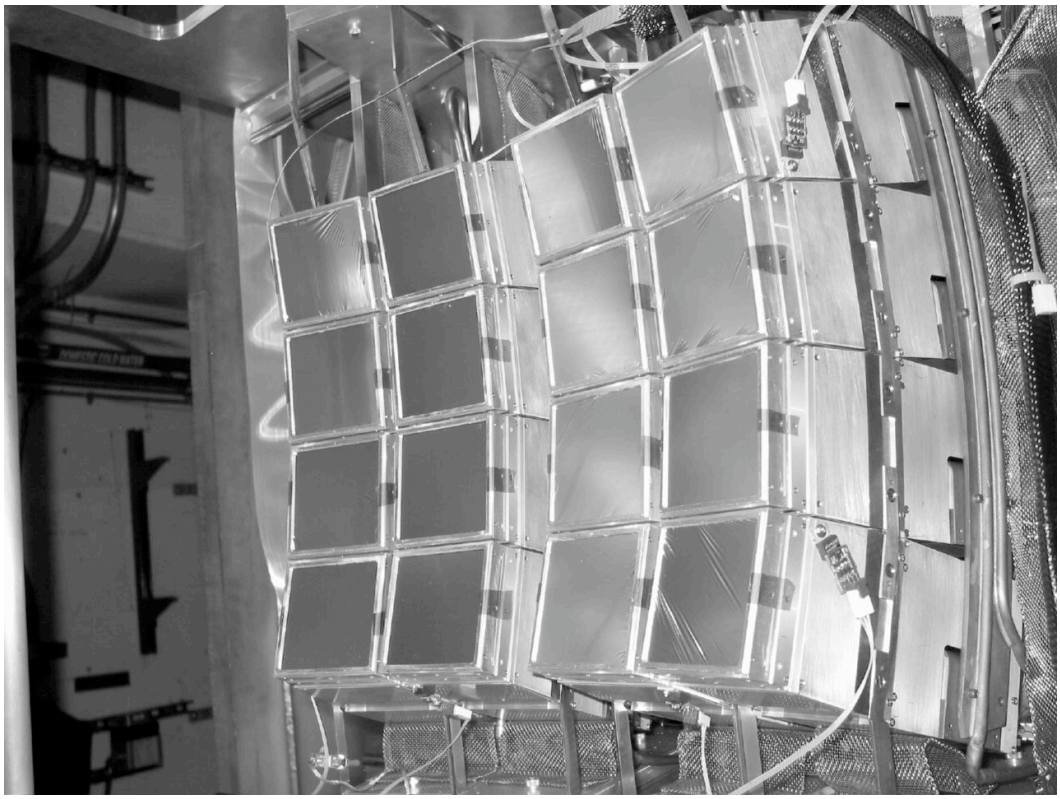

Fig. 1. An Image of 16 HiRA telescopes configured for transfer reaction experiments.

[21] JTEC Instruments, 32 Thompson Rd. Rochester, NY 14623.

[22] A. Rogers, et al. manuscript in preparation.

[23] I. Wiedenhöver, M. Steiner, D. J. Morrissey, B. M. Sherrill, D. Bazin, J. Stetson, A. Stolz, O. Tarasov, J. Yurkon, the NSCL staff, Commissioning of the new a1900 high-resolution high-acceptance fragment separator at the coupled cyclotron facility, AIP Conference Proceedings **610** (2002) 937–941.

[24] D. J. Morrissey, B. M. Sherrill, M. Steiner, A. Stolz, I. Wiedenhoever, Commissioning the a1900 fragment separator, Nucl. Instr. and Meth. B **204** (2003) 90–96.

[25] A. Stolz, T. Baumann, T. N. Ginter, D. J. Morrissey, M. Portillo, B. M. Sherrill, M. Steiner, J. W. Stetson, Production of rare isotope beams with the nscl fragment separator, Nucl. Instr. and Meth. B **241** (2005) 858–861.

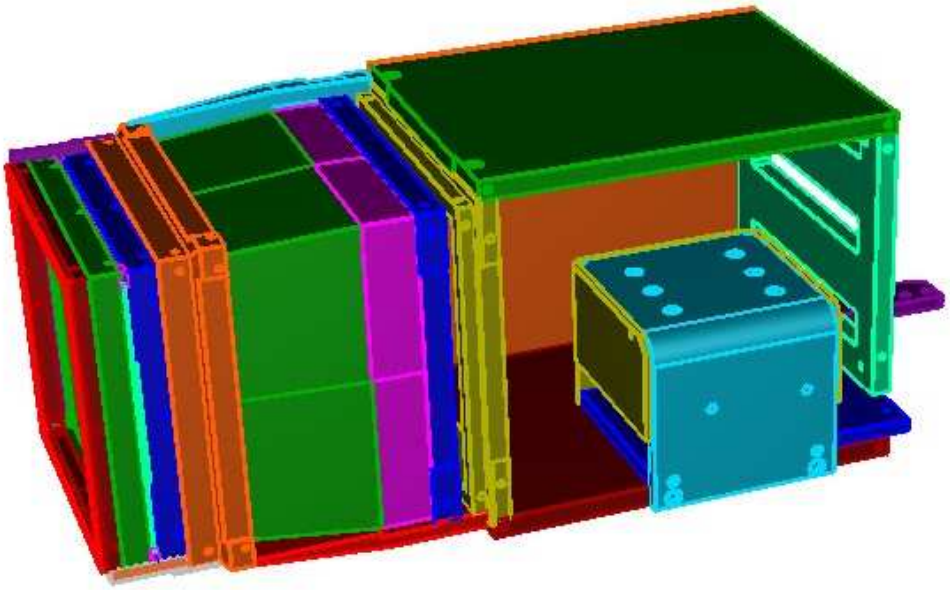

Fig. 2. A technical drawing of a single HiRA telescope.

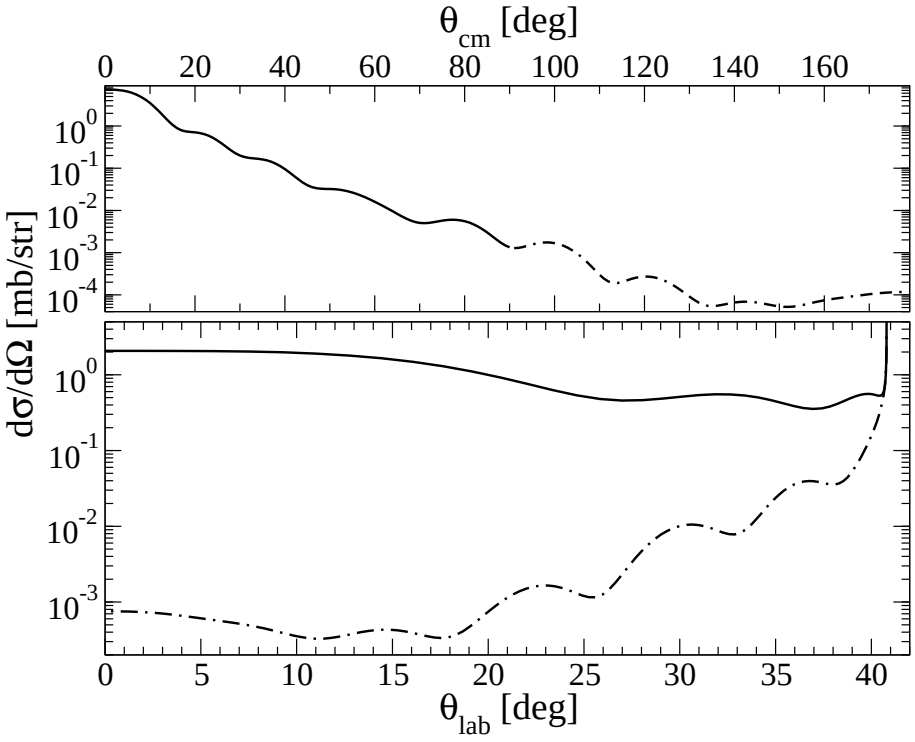

Fig. 3. The angular distributions for ^{65}Ge(p,d)^{64}Ge at E/A=60 MeV in the center of mass (top panel) and laboratory (bottom panel) frame.

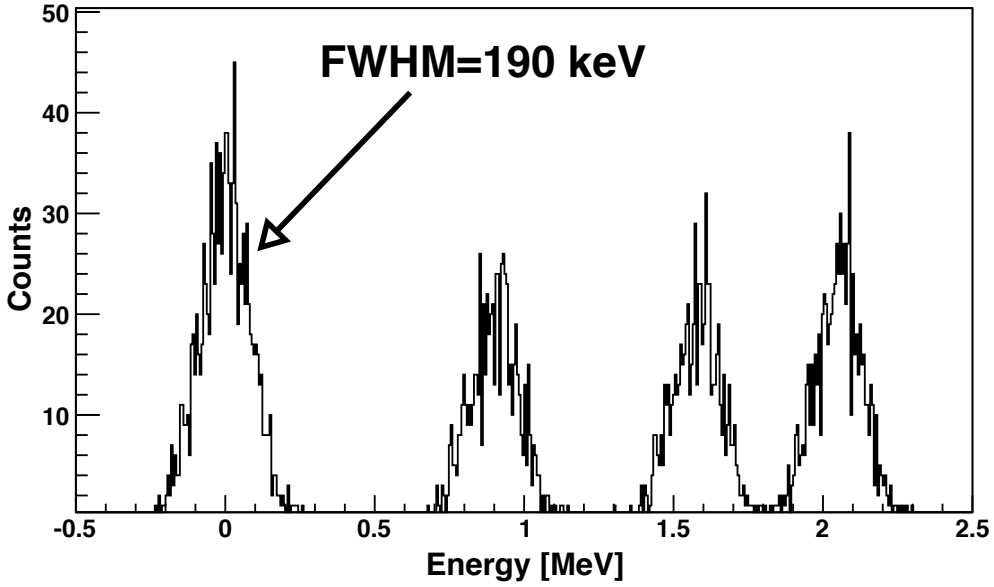

Fig. 4. A simulated excitation spectrum from a ^{65}Ge(p,d)^{64}Ge transfer reaction using HiRA.

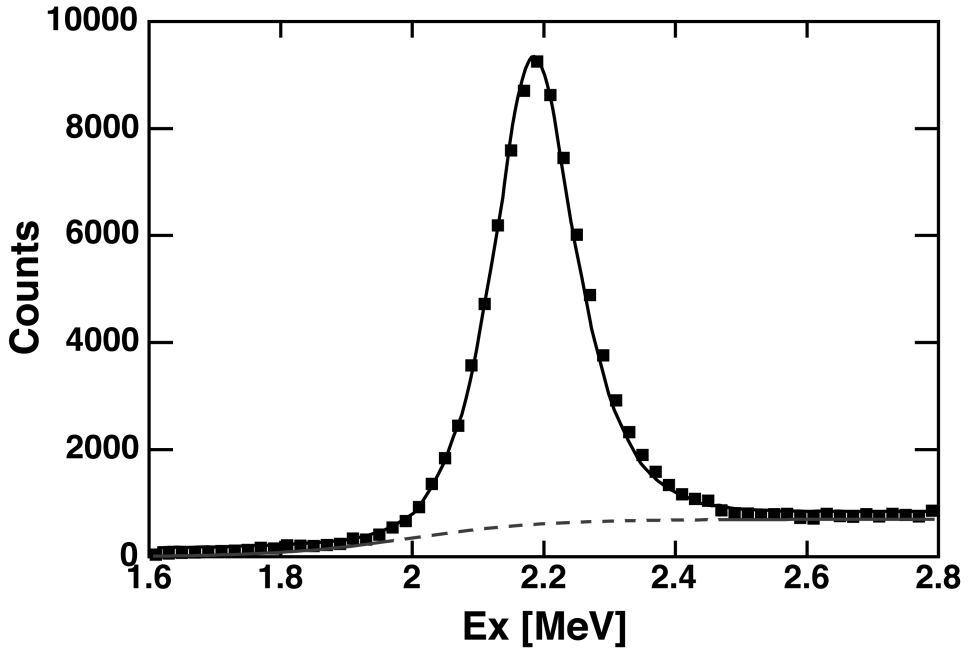

Fig. 5. The experimental excitation-energy spectrum of ^{6}Li derived from d-alpha pairs.

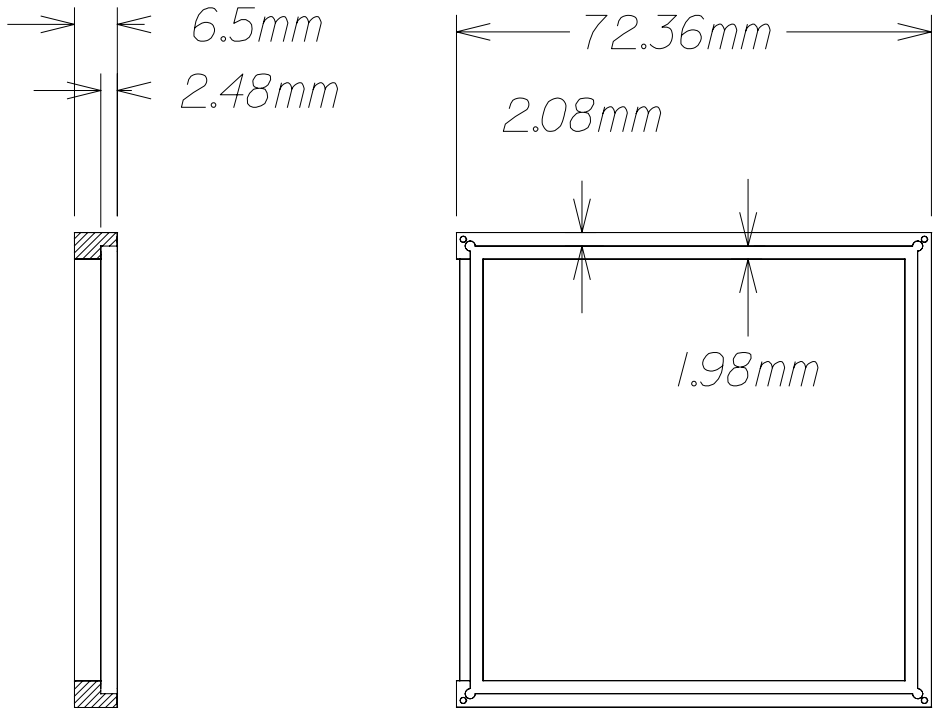

Fig. 6. A technical drawing of the HiRA silicon frame.

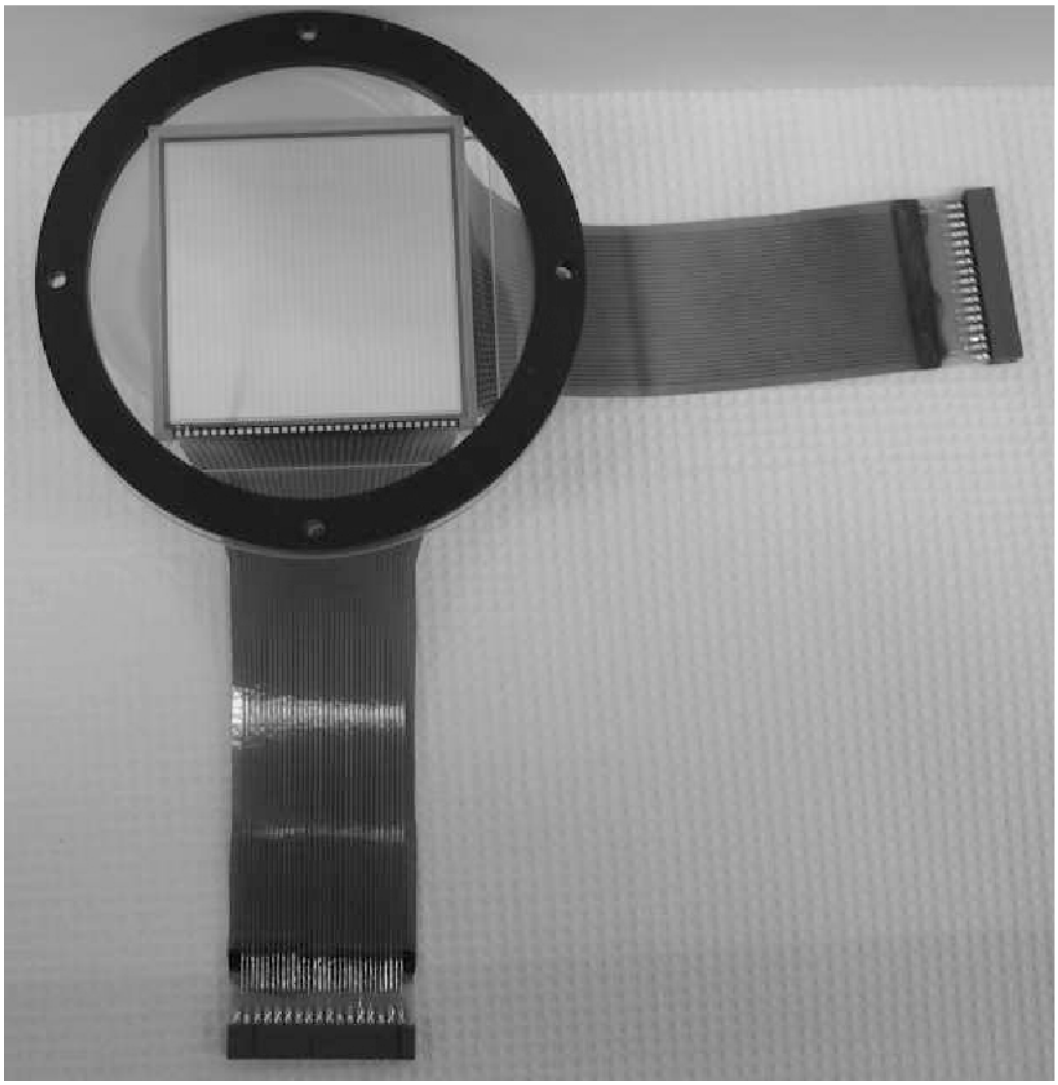

Fig. 7. An image of a HiRA double sided silicon strip-detector.

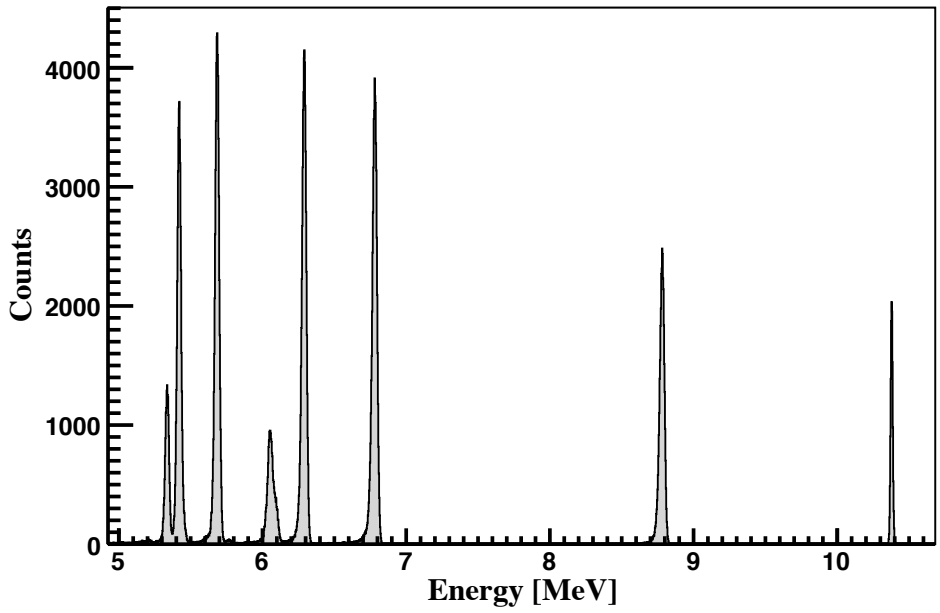

Fig. 8. A ^{228}Th spectrum for a single strip of a HiRA double-sided silicon strip-detector.

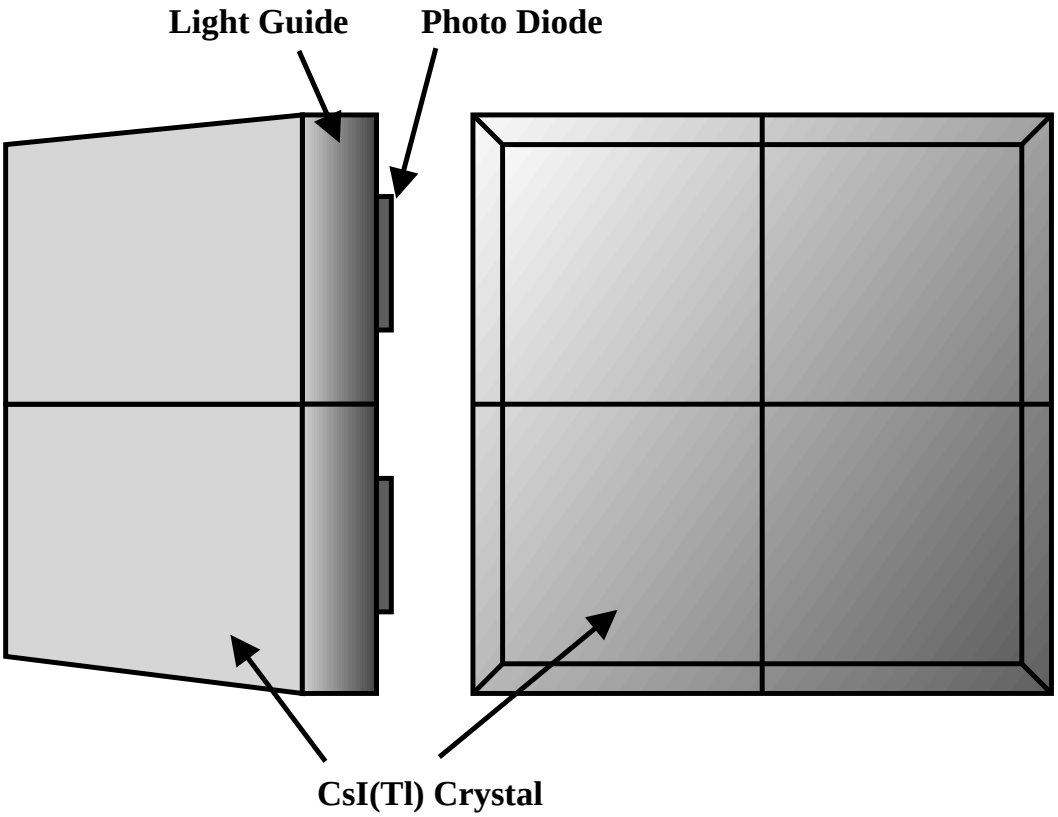

Fig. 9. A drawing of the HiRA CsI(Tl) crystals.

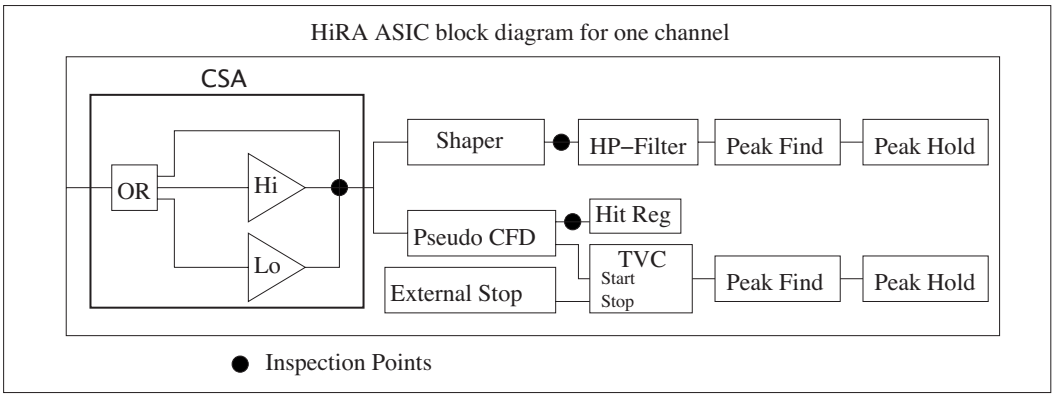

Fig. 10. A diagram of one channel of the HiRA ASIC.

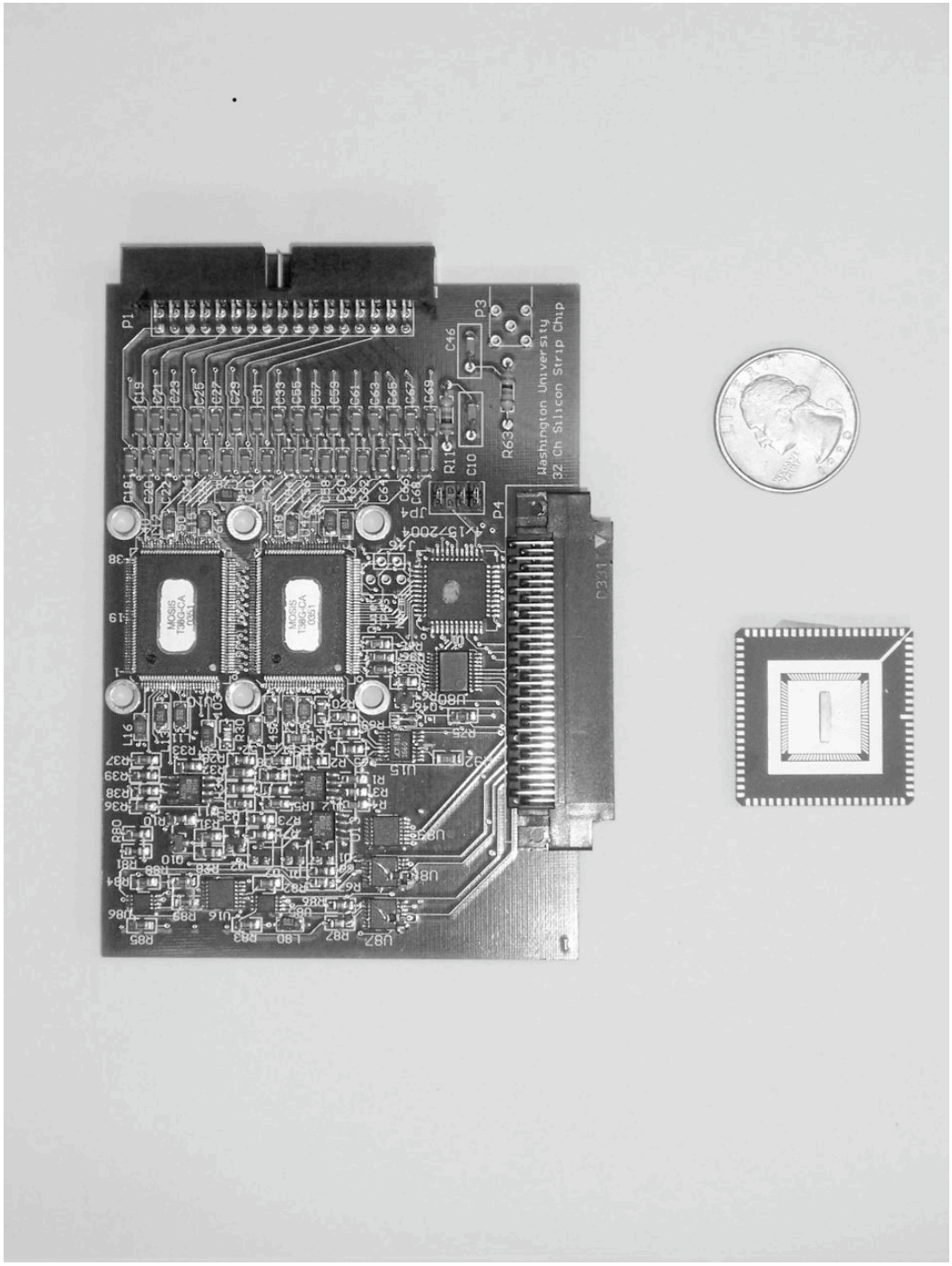

Fig. 11. Image of a HiRA chip-board and a protoype chip with a quarter for reference.

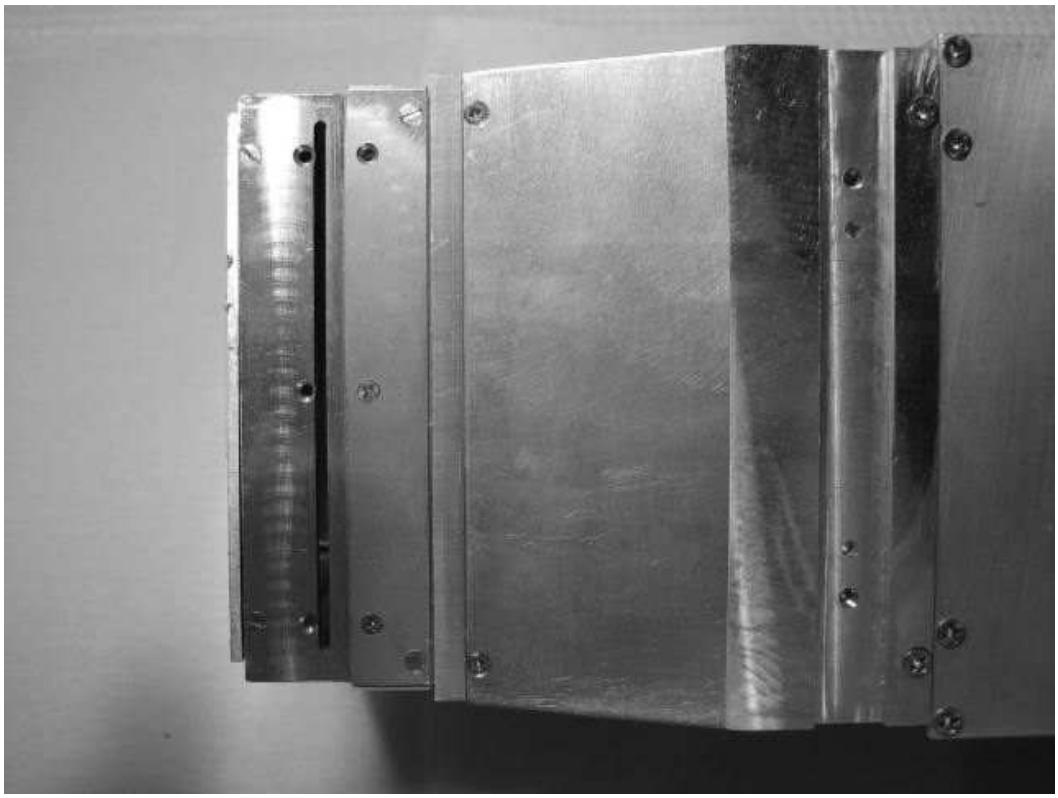

Fig. 12. An image of the side of a HiRA telescope showing the insertion slot for alpha calibrations.

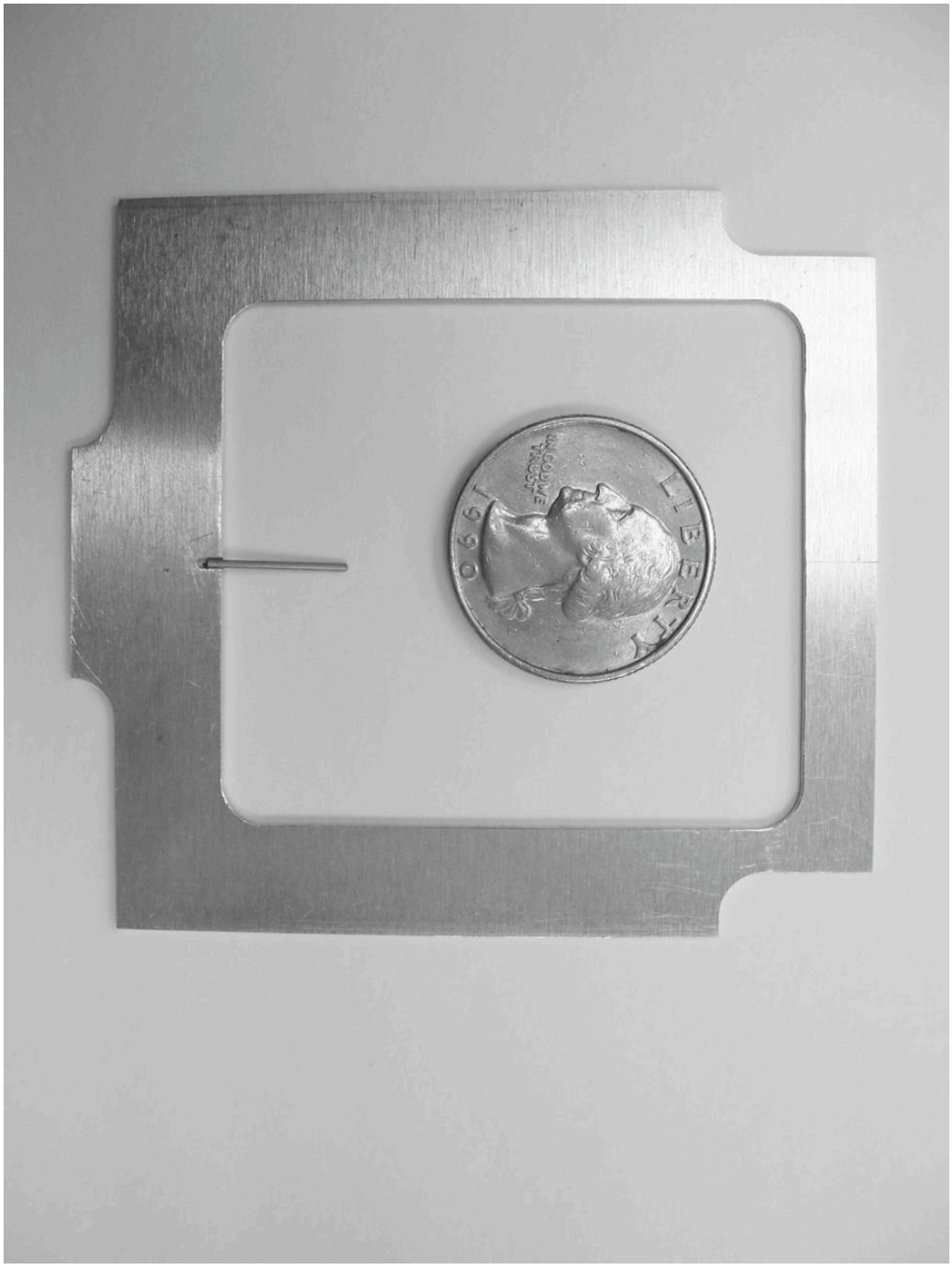

Fig. 13. An image of the alpha calibration source frame and source pin.

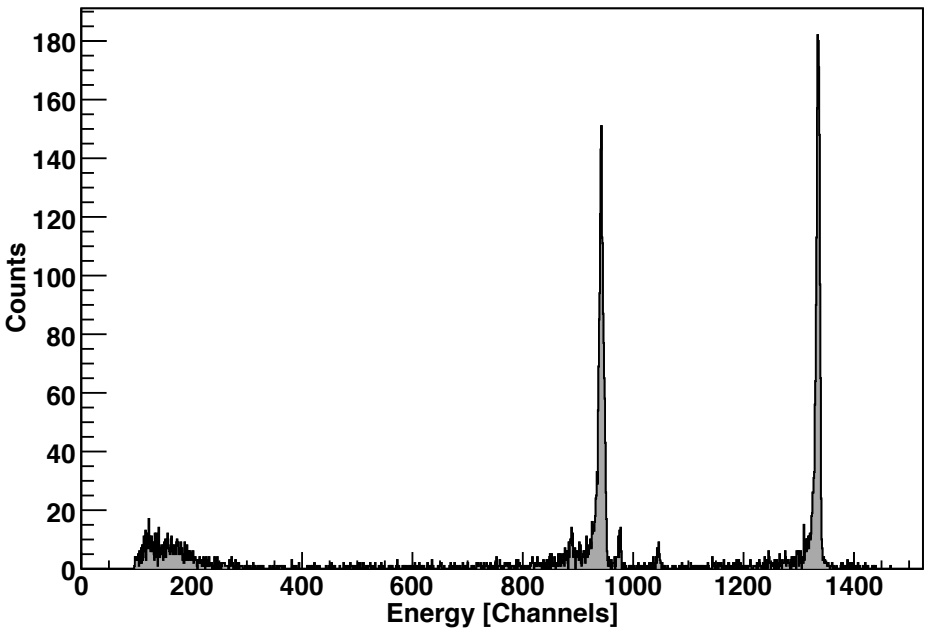

Fig. 14. An energy spectrum from the pin source gated on the 16th strip on EF and the 16th strip on EB.

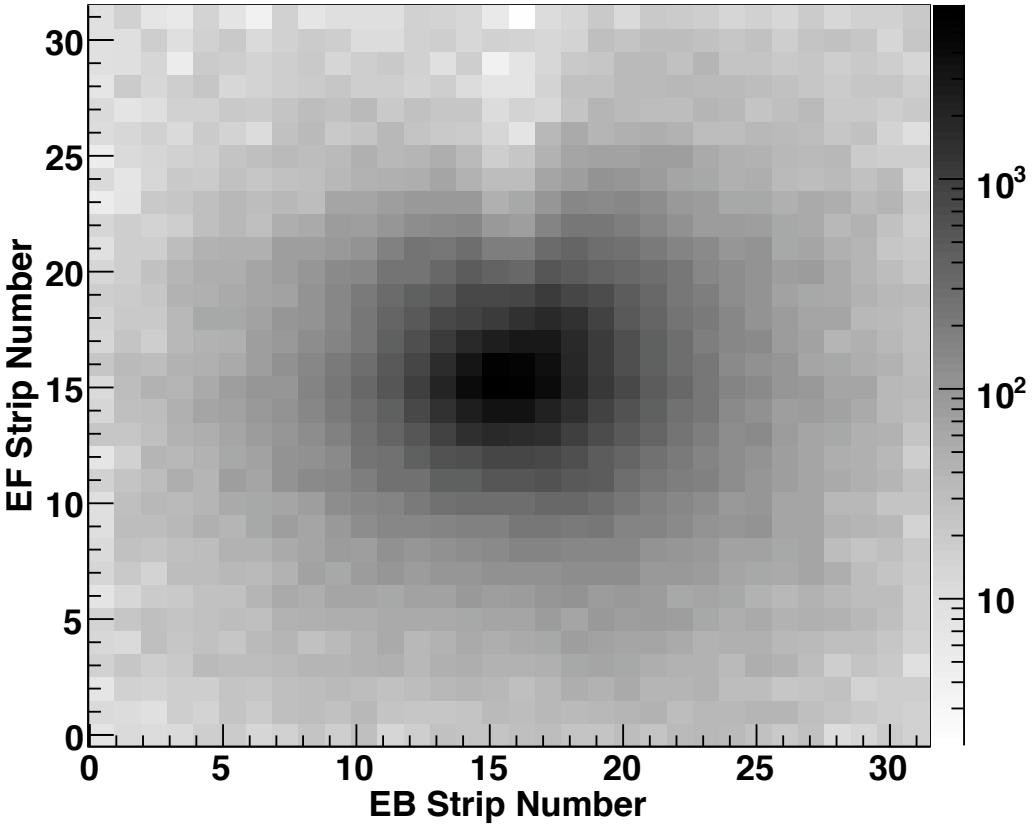

Fig. 15. The 2-dimensional hit pattern from a pin source inserted between the two silicon detectors of a HiRA telescope.

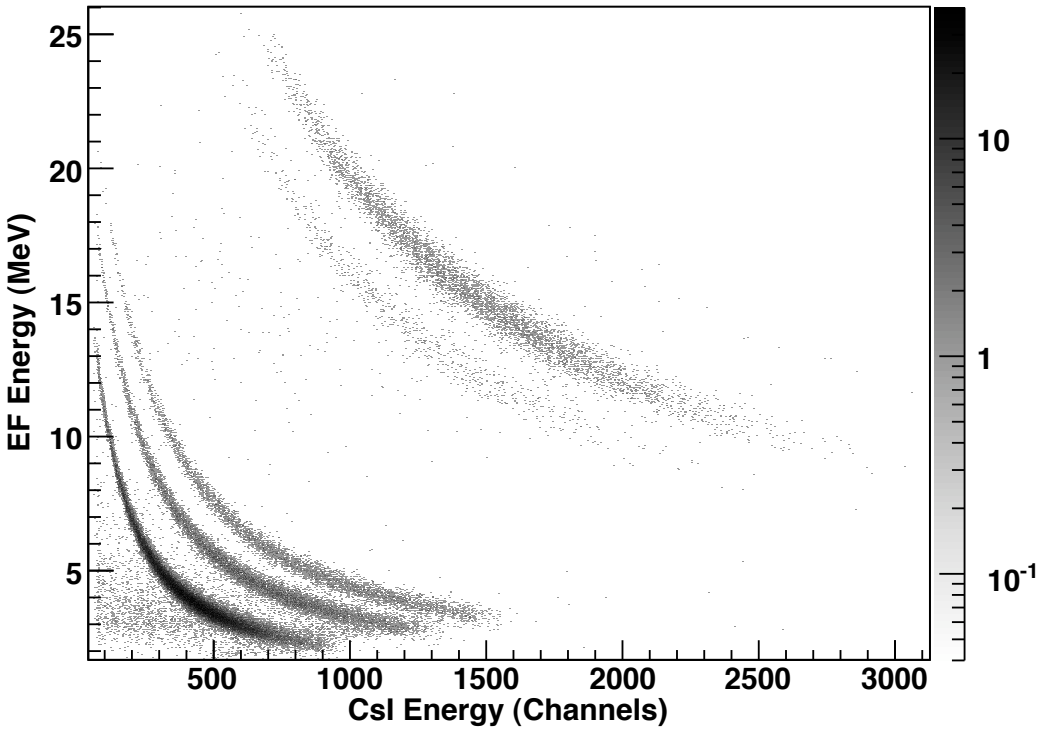

Fig. 16. A PID spectrum using the CsI and thick silicon.

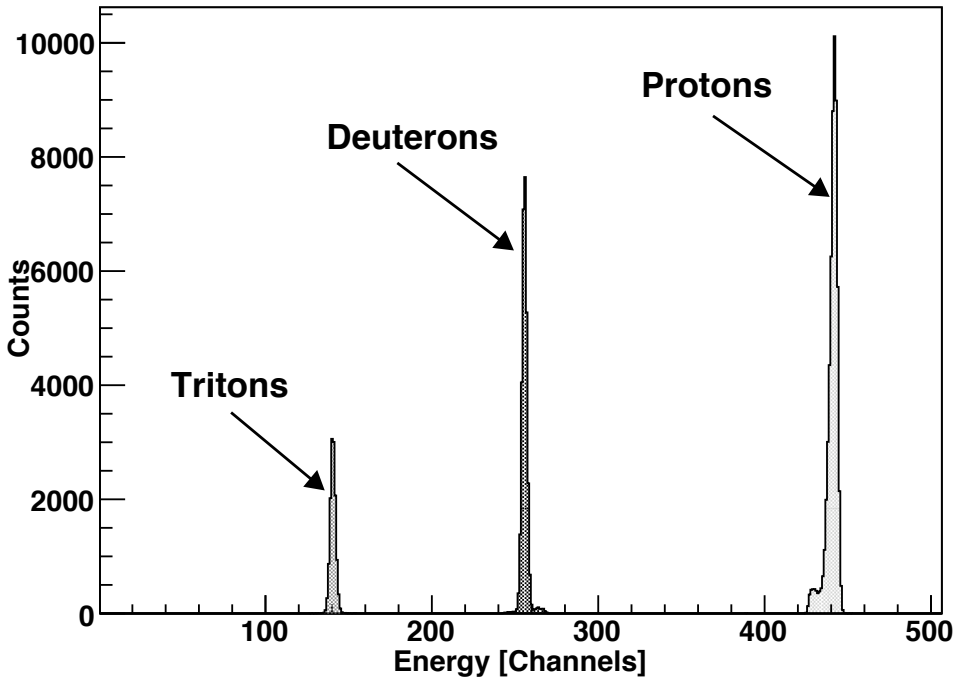

Fig. 17. Calibration spectrum for CsI(Tl) using elastic scattering of light charged particles.

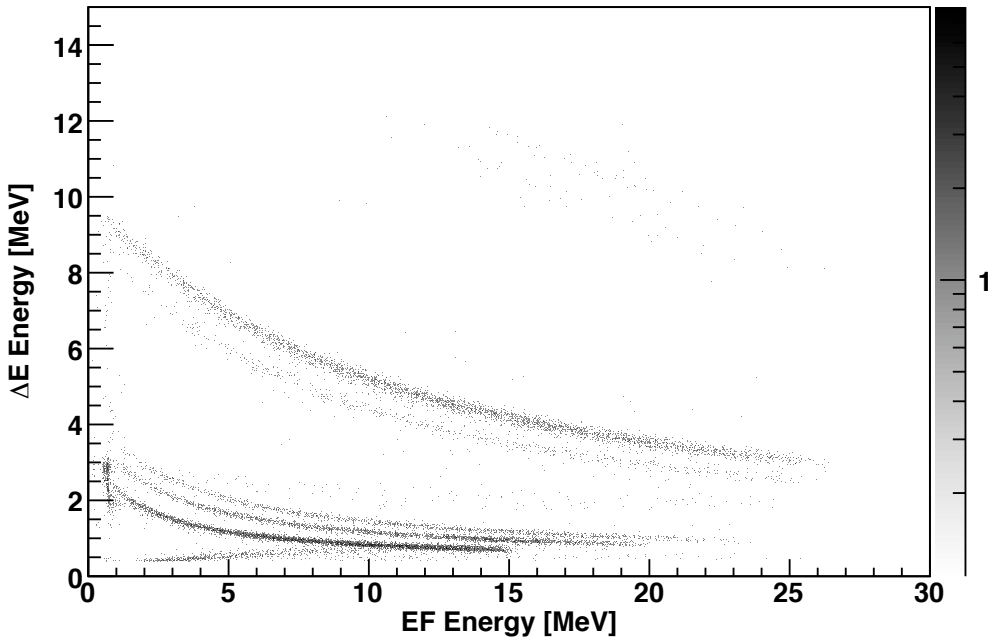

Fig. 18. A PID spectrum using both silicon detectors.